Inner-electron ionization of Sr $5s16l$ states

H. Maeda and T. F. Gallagher
Department of Physics, University of Virginia, Charlottesville, Virginia 22904-0714
(Received 15 November 2001; published 19 April 2002)

We have measured the probability of inner-electron ionization (IEI) of Sr $5s16l$ atoms when exposed to intense 230-fs laser pulses. We find that the probability of IEI rises sharply at $l=5$ and is approximately equal to one for $l>5$. For $l=5$ the classical inner-turning point is at $15a_0$, far greater than the size of the Sr^+ ionic core, ruling out core penetration as the factor governing inner-electron ionization. For the Sr $5p_{1/2}16l$ states of $l>5$ the autoionization lifetime, which is due to the electrostatic interaction between two-valence electrons, is greater than the Kepler orbit time. These comparisons suggest that both inner-electron ionization and autoionization are governed by long-range electrostatic interactions.

DOI: 10.1103/PhysRevA.65.053405 PACS number(s): 32.80.Rm

I. INTRODUCTION

Photoionization of multielectron atoms, even two-electron atoms, is a problem of long-standing interest. If the initial state is the ground state, there are two parts to the problem; it is not clear which electron acquires energy from the light, nor is it clear how the energy will be shared among the electrons subsequent to the absorption of the light. If the initial state is an excited state, however, it is often true that one electron plays a dominant role in the absorption of the photon, substantially simplifying the problem and allowing us to unambiguously address the question of how the energy is partitioned subsequent to absorption of the light.

An interesting excited-state photoionization process in two-valence-electron atoms is inner-electron ionization (IEI) of bound Rydberg states [1,2]. The essential idea is easily understood using the Ba $6snd$ Rydberg states as an example. When Ba $6snd$ Rydberg atoms are exposed to intense, short, e.g., 5 ps in the experiments of Stapelfeldt *et al.* [1], laser pulses, the inner $6s$ core electron is ejected from the atom while the outer nd Rydberg electron remains a spectator and is projected onto Ba^+ Rydberg states, the highest lying having the same size as the orbit of the initial $6snd$ Rydberg state. This process is observed to occur only if the duration of the laser pulse τ_L is shorter than the classical Kepler orbit time, $\tau_K=2\pi n^3$ (a.u.), of the Rydberg electron [1].

Why IEI occurs when it does, for $\tau_L<\tau_K$, was originally explained using a time-domain picture [1,2]. If $\tau_L<\tau_K$, for some of the $6snd$ atoms the nd Rydberg electron does not come near the ionic core during the laser pulse, and in these atoms the Rydberg electron remains a spectator while the inner $6s$ electron is ejected by multiphoton ionization. If the $6s$ electron is ejected suddenly compared to the orbit time of the Rydberg electron, it is reasonable to suppose that the nd Rydberg electron is projected onto the Ba^+ Rydberg states, with the most probable principal quantum number $n_{II}=\sqrt{2}n_I$ (where $n_I\equiv n$). If, on the other hand, the Rydberg electron comes near the core during the laser pulse, the two electrons interact during the laser pulse, and it is likely that the loosely bound Rydberg electron will be ejected from the atom, with the result that no Ba^+ Rydberg states are formed. A recent experiment using a Sr $5snd$ Rydberg wave packet by Maeda *et al.* [3] has shown this picture to be basically correct. When the nd electron is far from the core, IEI occurs and Sr^+ Rydberg states are produced, but when the nd electron is near the core it does not.

Although the wave-packet experiment shows that the time-domain picture is essentially correct, it is not completely so. At high n, with 5-ps pulses, when $\tau_L<\tau_K$ Stapelfeldt *et al.* observed IEI [1], but with 200-fs pulses Tate and Gallagher only observed IEI from Ba $6snd$ states when $\tau_L<2\tau_K$ [4], contrary to the observation of Stapelfeldt *et al.* Furthermore, in the wave-packet experiment by Maeda *et al.* the observed final Sr^+ Rydberg state distribution does not match what would be expected if the Rydberg electron were simply projected onto the Sr^+ final states. The final states are lower-lying states than expected [3].

In all the discussion above we have considered IEI starting from states in which the Rydberg electron is in an nd orbit. However, if the outer Rydberg electron is in a high-angular-momentum state, so that it never comes near the ionic core, IEI would be possible even though $\tau_L\gg\tau_K$. In fact, Rosen *et al.* observed IEI of states of n ranging from $25<n<48$ and $l\approx10$ by single photon absorption when they exposed Sr $5fnl$ atoms to nanosecond pulses of $\sim$550-nm light [5]. In this case $\tau_L\approx2600\tau_K$. We can estimate the inner radial-turning point r_i for a Rydberg state, which has a vanishingly small binding energy, by equating the centrifugal barrier to the coulomb potential, which yields

$$r_i=l(l+1)/2, \tag{1}$$

in a.u. [6]. For $l=10$ Eq. (1) gives a value of $55a_0$, where a_0 is the radius of first Bohr orbit, so the $l=10$ Rydberg electron of the $5fnl$ atom never comes at all close to the ionic core, and the fact that $\tau_L\gg\tau_K$ is therefore irrelevant. A second interesting point about the experiment of Rosen *et al.* is that they excite the inner $5f$ electron to an energy just above the Sr^{2+} ionization limit, so that it does not leave the atom suddenly, and the inner electron is not projected onto the Sr^+ Rydberg states. Instead of observing $n_{II}\approx\sqrt{2}n_I$ they observed $n_{II}\approx n_I$, which they attribute to long-range electrostatic interaction between the two electrons [5].

The fact that IEI does occur from $l=10$ states with long laser pulses is not surprising, but it does raise the following

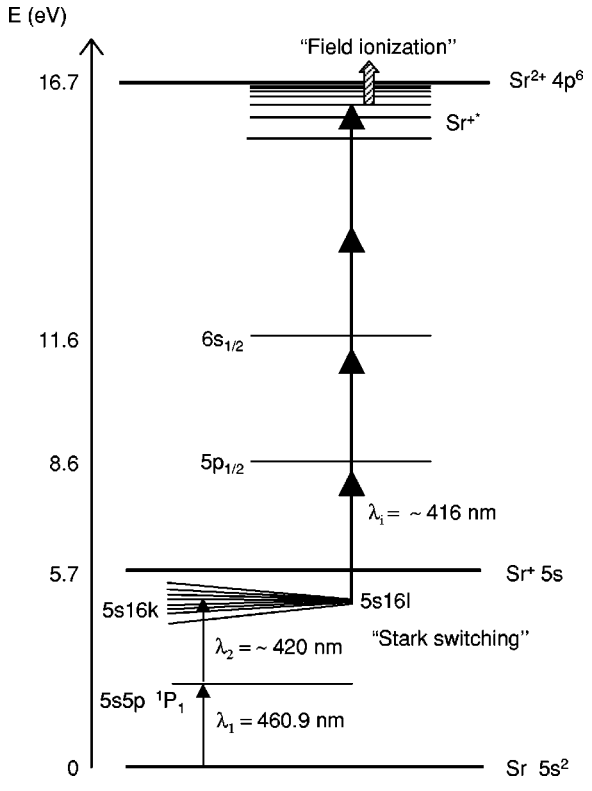

FIG. 1. Excitation and ionization scheme of Sr $5s16l|m|=1$ states.

question: Does the outer electron need to penetrate the core or merely come close enough for an electrostatic interaction to suppress IEI? In other words, is this interaction responsible for the fact that IEI does not always occur for $\tau_L < \tau_K$? To address these questions we have examined the l dependence of IEI from Sr $5snl$ states. In the following sections we describe our experimental approach, our observations, and the conclusions we draw from them.

II. EXPERIMENT

A. General

The essence of our experiment is shown in the energy-level diagram of Fig. 1. We use the Stark-switching technique [7] to produce the Sr $5s16l$ states. Specifically, using two 5-ns laser pulses we excite Sr atoms in an electric field from the ground state to a $5s16k$ Stark state, where k is the Stark quantum number. The first dye laser drives the $5s^2\,{}^1S_0$-$5s5p\,{}^1P_1$ transition at $\lambda_1 = 460.9$ nm [8], and the second one drives the $5s5p\,{}^1P_1$-$5s16k$ transition at $\lambda_2 \sim 420$ nm [9]. The electric field is turned off slowly, and the $5s16k$ state evolves adiabatically to the zero field $5s16l$ state to which it is adiabatically connected. Once the atoms are in the $5s16l$ state we can ionize them in one of two ways. First, we can drive the IEI transition by exposing the Sr $5s16l$ atoms to an intense, 230-fs, 416-nm pulse. To detect that IEI has occurred, we monitor the Sr^+ Rydberg ions (which we denote by $Sr^{+}*$) by field ionization. Second, we can drive the isolated-core excitation (ICE) [10] $5s16l$-$5p_{1/2}16l$ transition at 422 nm with a 230-fs laser pulse of reduced intensity. In this case the resulting $5p_{1/2}16l$ atoms autoionize, producing low-lying states of Sr^+. Since it is straightforward to drive all atoms in the Sr $5s16l$ state to the Sr $5p_{1/2}16l$ state, we use ICE to determine the number of atoms in the initial $5s16l$ state. Irrespective of whether we are observing the IEI signal or the ICE signal we collect our experimental data by scanning the wavelength of the second dye laser, which drives the $5s5p$-$5s16k$ transition and populates a specific $5s16l$ state, and recording either the ICE or the IEI signal. By taking the ratio of the IEI signal to the ICE signal we obtain the relative probability of IEI as a function of l.

B. Details

A resistively heated oven produces an effusive atomic beam of Sr, which is collimated to ~ 1 mm diameter and passes between a pair of capacitor plates, A and B in Fig. 2, separated by a distance of 2.1 mm, where the atomic beam is crossed at nearly a right angle by three laser beams. The third harmonic of a pulsed Nd:YAG laser (where YAG represents yttrium aluminum garnet) operated at a 20-Hz repetition rate is used to pump two dye lasers to excite stepwise Sr from the $5s^2\,{}^1S_0$ ground state to highly excited $5s16k$ Stark states, via the $5s5p\,{}^1P_1$ intermediate state in an external field of up to 1250 V/cm, as shown by Fig. 1. The first dye laser, of the standard Littman configuration [11], is operated at a wave-

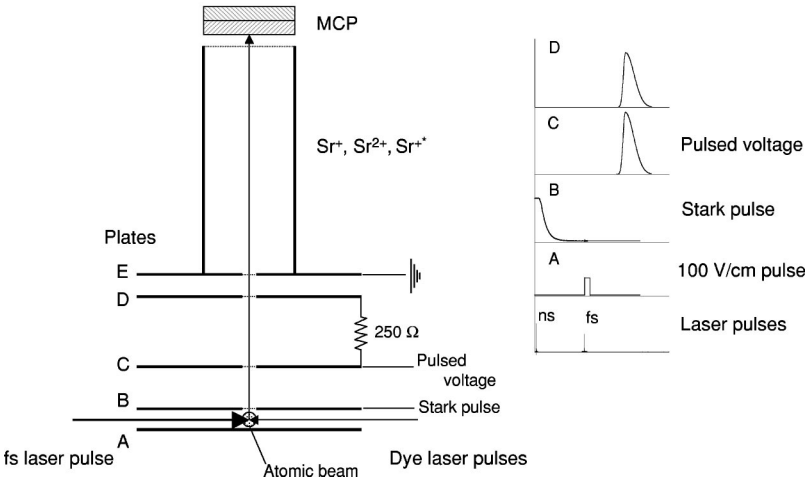

FIG. 2. Diagram of the interaction region and a timing sequence of electric fields applied to the plates A–E. See the text for details.

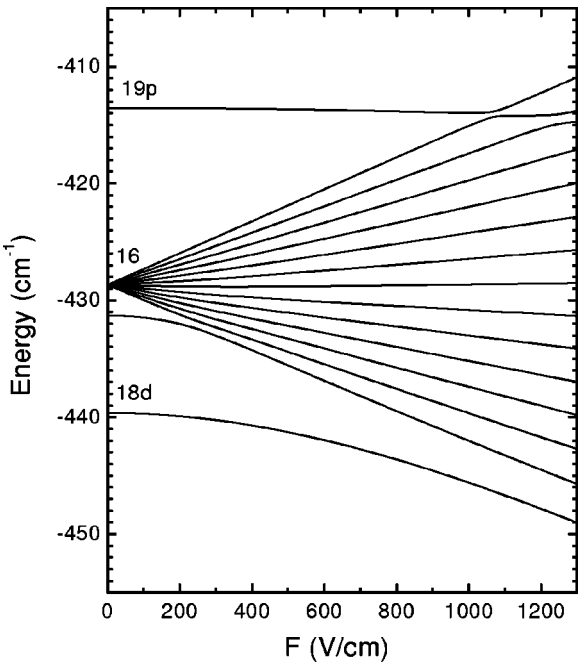

FIG. 3. Calculated Stark map of Sr $5s16l|m|=1$ states. Note that quantum defects of the states for $l>4$ are set to zero in this diagram.

length of 460.9 nm, and has a linewidth of less than ~ 0.66 cm^{-1}. The second dye laser is built in a dual grating Littman configuration [12], and its typical linewidth is estimated to be ~ 0.3 cm^{-1} in the present experiment. The second laser is scanned in wavelength around $\sim$ 420 nm to excite individual $5s16k$ Stark states from the $5s5p\ ^1P_1$ state [9]. Both dye lasers have a pulse width of ~ 5 ns at FWHM (full width at half-maximum). The polarizations of the two dye lasers are linear and perpendicular to each other, and the polarization of the second laser is parallel to the external electric field in order to excite $|m|=1$ states, as the structure of the Stark map of $|m|=1$ states is much simpler than that of $|m|=0$ states. Avoided crossings between the s state and other lower l states make the Stark-switching technique more delicate for $|m|=0$ states.

After excitation of the $5s16k$ Stark states of Sr in the external field, the field is reduced to zero slowly enough that the $5s16k$ state passes adiabatically to a $5s16l$ Rydberg state in zero field. As can be seen in Fig. 3, a Stark map of the Sr $5s16k$ $|m|=1$ manifold, there are only two avoided crossings below the field strength $F=1250$ V/cm; one between the $l=15$ and $l=1$ states at $F\approx 1070$ V/cm, whose energy separation is ~ 0.5 cm^{-1} and the second between the $l=14$ and $l=1$ states at $F\approx 1230$ V/cm with a 1 cm^{-1} separation. Hence we only need to pay close attention to controlling the slew rate near zero field, where the Stark states are most nearly degenerate. Following the method of Pruvost *et al.* [13], we first reduce the field strength F by approximately 95% of its initial value in 1 μs of switching time, and then reduce the residual field to zero in the following ~ 2.5 μs to fulfill the adiabatic condition near zero field. The upper limit to the slew rate of this slowly relaxing field is determined from the energy spacing ΔW between the highest $l=15$ and the second highest $l=14$ states and from the adiabatic condition $dW/dt<\Delta W^2$. We estimate the energy spacing of very high-l states of the $n=16$ manifold based on the assumption that quantum defects of such high-l states originate mainly from the adiabatic-dipole-core polarizability of the Sr^+5s core [7,14]. We estimate that the fastest allowed slew rate near zero field is 50 V/cm/μs, which is higher than our experimental rate of 3 V/cm/μs. The Stark field is applied to the upper plate *B*, whereas a small voltage is constantly applied to the lower plate *A* to compensate for a small offset voltage of the Stark-switching device and ensure that the IEI laser is fired at zero field. The residual electric field is estimated to be less than 50 mV/cm.

When the field reaches zero, the excited Sr atoms are in the $5s16l$ state and we further excite them by IEI or ICE. In IEI an intense, short laser pulse irradiates the Sr $5s16l$ atoms to multiphoton ionize the $5s$ core electron. This ionization laser pulse is obtained from a continuous-wave, self-mode-locked Ti:Al_2O_3 laser which is amplified by a regenerative amplifier running at a 20-Hz repetition rate to produce 2-mJ, 230-fs (FWHM) pulses at 832 nm. The output of the femtosecond laser system is frequency doubled by a 0.5-mm-long β-barium borate (Type I) crystal to 416 nm, which is nearly resonant with the $Sr^+5s_{1/2}$-$5p_{1/2}$ transition at 422 nm [8], so that it becomes possible to efficiently multiphoton ionize the inner electron and produce highly excited Rydberg ions, Sr^+* [3]. We note that the laser wavelength of 416 nm is deliberately detuned from the $Sr^+5s_{1/2}$-$5p_{1/2}$ core transition at 422 nm to avoid populating the $5p16k$ states during the Stark-switching time of ~ 3.5 μs by an ICE from the $5s16k$ states. If the wavelength is set to the resonance at 422 nm the weak train of pulses leaking from the regenerative amplifier drives the $5s16k$-$5p16k$ transition while the Stark-switching field is still present. The 416-nm light is focused by a 500-mm focal length lens, giving a peak intensity of $\sim 2\times 10^{13}$ W/cm^2.

Approximately 40 ns after the irradiation by the femtosecond laser pulse, a 30-V positive voltage pulse of 10-ns rise time is applied to field plate *A* in Fig. 2, providing approximately a 100-V/cm field to push the ions produced, Sr^+,Sr^{2+}, and Sr^+*, out of the interaction region between capacitor plates *A* and *B* through a grid in the center of the plate *B* into a second field region defined by plates *C* and *D*, which are separated by 10 mm. Note that the 100-V/cm field is insufficient to field ionize the bound Sr Rydberg atoms. After all ions produced have moved into the second field region, an adjustable pulsed positive voltage (0–12 kV) of 500-ns rise time is applied to plate *C* and indirectly to plate *D*, through the 250 Ω resistor, so there is only a small field applied to the ions while they are between plates *C* and *D*. The primary purpose of the second field region is to keep the Sr^+* ions in a relatively low field during the 500-ns rise time of the field-ionization pulse. These ions pass through the aperture of plate *D* after a 450-ns flight time. Since plate *E* is grounded and is 4 mm from plate *D*, the field in the third region, between these plates, is up to 30 kV/cm. We estimate the minimum required threshold field for ionization of the Sr^+* ions using $n_{\mathrm{II}}=\sqrt{2}n_{\mathrm{I}}$ and $F_{th}=8/16n_{\mathrm{II}}^4$ (a.u.)

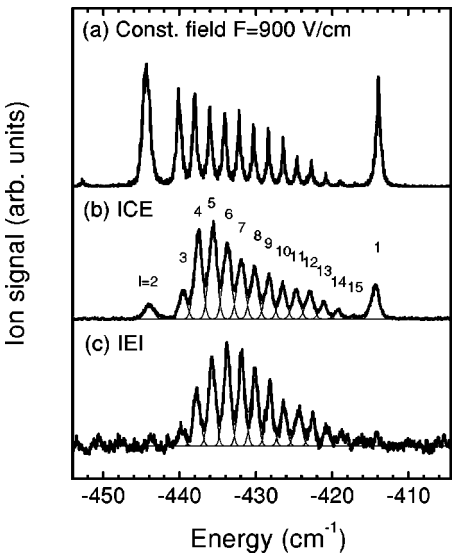

FIG. 4. Typical trace of (a) a field-ionization signal of the $5s16k$ Stark states excited in a constant 900-V/cm external field, (b) autoionizing ICE signal of the $5p_{1/2}16l$ states excited from the $5s16l$ states, which are populated using the Stark-switching technique, and (c) IEI signal from the $5s16l$ Rydberg states populated by the same Stark-switching scheme applied to the ICE measurement, plotted against the wavelength λ_2 of the second dye laser. In all cases excitation of the $5s16k$ Stark states takes place in the external field of $F=900$ V/cm. Thin curves given in (b) and (c) are deconvoluted peak intensities of each of the states.

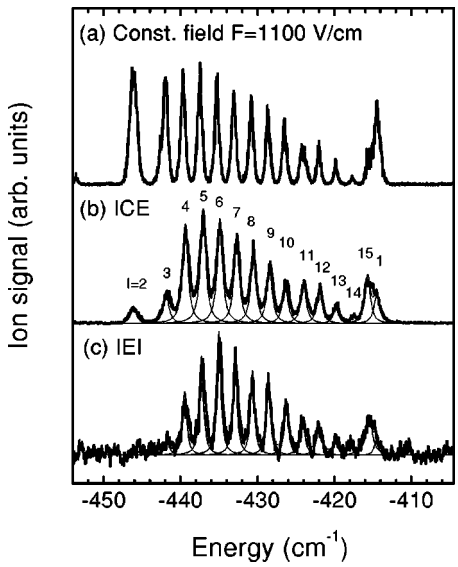

FIG. 5. Typical trace of (a) a field ionization signal of the $5s16k$ Stark states excited in a constant 1100-V/cm external field, (b) autoionizing ICE signal of the $5p_{1/2}16l$ states excited from the $5s16l$ states, which are populated using the Stark-switching technique, and (c) IEI signal from the $5s16l$ Rydberg states populated by the same Stark-switching scheme applied to the ICE measurement, plotted against the wavelength λ_2 of the second dye laser. In all cases excitation of the $5s16k$ Stark states takes place in the external field of $F=1100$ V/cm. Thin curves given in (b) and (c) are deconvoluted peak intensities of each of the states.

≈ 10 kV/cm. In the third field region, Sr^{+}* Rydberg ions are field ionized to produce Sr^{2+}, and all ions are accelerated toward the microchannel plate detector. After the high-field third region the ions pass through an 80-mm-long, field-free drift region. Strontium single ions, Sr^{2+} ions, and field-ionized Sr^{+}* reach the detector at different times and are detected separately. To record the IEI signal, we use a boxcar integrator, set its gate to the Sr^{+}* time-of-flight (TOF) signal, and record the signal intensity as a function of the wavelength of the second dye laser [see Figs. 4–6(c)].

To obtain the information of relative initial-state population distribution of the $5s16l$ state, we separately measure the ICE signal of each angular momentum state. To detect ICE signal we simply retune the femtosecond laser from 416 nm to 422 nm, which matches the Sr^{+} $5s$-$5p_{1/2}$ core transition. In addition, we use a combination of a $\lambda/2$ plate and a polarizer to reduce the laser intensity to avoid any saturation effects and multiphoton production of Sr^{2+}. With this approach there is no sign of populating the $5p16k$ states due to the small leakage light from the regenerative amplifier, as mentioned previously. The photoionization signal resulting from autoionization of the final $5p16l$ states is recorded against the second dye-laser wavelength by setting a boxcar gate on the Sr^{+} TOF signal [see Figs. 4–6(b)]. Taking the ratio of the IEI signal intensity to that of the ICE signal gives us the relative IEI probability of each l state within the $n=16$ manifold (see Fig. 7). It is also informative to record field-ionization spectra of the $5s16k$ Rydberg Stark states in a constant electric field with no time delay after the second laser pulse to determine how many atoms we excite to the states in the $n=16$ manifold before Stark switching. Typical traces are shown in Figs. 4–6(a).

Finally, we also detect the IEI signal of Sr Rydberg states in zero field to measure the IEI probability of the s state, because in the experiments described above we focus on measuring IEI probability of the $|m|=1$ states. Note that the polarizations of two dye lasers are not changed in the zero-field measurements, i.e., they are still nominally perpendicular to each other. However, the incomplete perpendicularity of the laser polarizations allows us to observe a small yet measurable signal originating from the s state as well as the large signal from the d state. In this case the initial-state population is determined by field ionizing the Rydberg states instead of detecting the ICE signal. We determine the relative IEI probability of the s state against the d state in zero field, and plot the results in Fig. 7 by normalizing the IEI probability of d state obtained in the zero-field experiment to that obtained in the Stark-field experiment.

III. OBSERVATIONS

As mentioned in the preceding section, we collect our data by recording different signals as the wavelength of the second laser is scanned. Typical data are shown in Fig. 4, taken with a field of $F=900$ V/cm. In Fig. 4(a) we show the spectrum obtained with the electric field left on after the first two dye-laser pulses and the excited atoms are field ionized with a pulsed field applied after the laser pulses. In other words, Fig. 4(a) is the excitation spectrum of the $5s16k$ Stark states. Figure 4(b) shows the spectrum obtained when

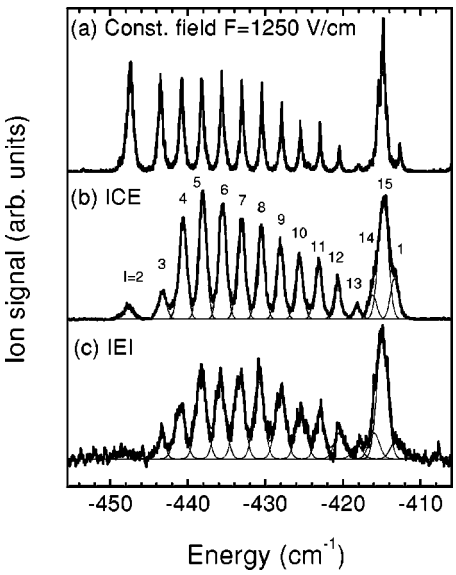

FIG. 6. Typical trace of (a) a field-ionization signal of the $5s16k$ Stark states excited in a constant 1250-V/cm external field, (b) autoionizing ICE signal of the $5p_{1/2}16l$ states excited from the $5s16l$ states, which are populated using the Stark-switching technique, and (c) IEI signal from the $5s16l$ Rydberg states populated by the same Stark-switching scheme applied to the ICE measurement, plotted against the wavelength λ_2 of the second dye laser. In all cases excitation of the $5s16k$ Stark states takes place in the external field of $F=1250$ V/cm. Thin curves given in (b) and (c) are deconvoluted peak intensities of each of the states.

the 900-V/cm electric field is switched off after the second laser pulse and the femtosecond ICE laser pulse arrives ~ 3.5 μs after the second laser pulse, when the field has reached zero. This spectrum represents the population in the $5s16l$ states ~ 3.5 μs after excitation by the first and second laser pulses. In Fig. 4(b) it is quite apparent that the population, which is transferred to low-l states, is diminished, due to radiative decay, relative to the population in the initially excited $5s16k$ states shown in Fig. 4(a).

In Fig. 4(c), we show the spectrum obtained when the femtosecond laser has the same delay, ~ 3.5 μs relative to the second laser, as in Fig. 4(b), but is tuned to 416 nm, with a peak intensity of $\sim 2\times 10^{13}$ W/cm^2, so as to effect IEI. Inspecting Figs. 4(b) and 4(c), we can see that for $l>5$ the IEI signal mirrors the population in the $5s16l$ states when the IEI pulse arrives, but for lower l the IEI signal is relatively lower. The data shown in Fig. 4 are typical of the data recorded with three different static fields of $F=900$,1100, and 1250 V/cm, as shown in Figs. 4, 5, and 6, respectively.

For each of the $5s16l$ states we have taken the ratio of the areas of the signals shown in Figs. 4–6to determine the relative probability of IEI. For high l it would be reasonable to consider that IEI occurs with 100% probability, and we could therefore normalize the signals at high l to 1. In Fig. 7 we show the average IEI probability vs l constructed using all our data taken in this experiment. Figure 7 shows in a more quantitative way what is suggested by Figs. 4–6, that IEI becomes very probable for $l>5$.

The IEI spectra shown in Figs. 4–6 were all taken with an ionization field in the third field region of 30 kV/cm. While we did not make careful measurements of the field dependence of the IEI signal, we observed that the onset of the IEI signal (10% of its maximum value) occurs at 10 kV/cm, and it reaches a plateau at 20 kV/cm. Assuming adiabatic ionization, these two fields imply that $19\leqslant n_{II}\leqslant 22$. This range of values is reasonable for projection of the initial Rydberg state onto the ionic Rydberg states. The IEI spectra of Figs. 4–6, taken with an ionization field of 30 kV/cm, show the entire IEI signal.

In addition to the observations shown using the Sr $5s16l$ states we have used the $5s17l$ states as well and obtained similar, but not as extensive, results. To demonstrate an interesting n scaling would necessitate using a large range of n values, at least five. Going to higher n requires better laser resolution and going to lower n requires switching much higher fields, both of which present substantial technical obstacles.

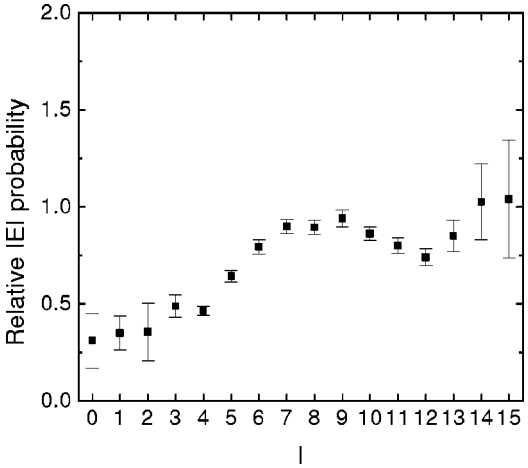

FIG. 7. Plots of the ratio of signal strengths of each angular momentum states obtained in the IEI measurements to those obtained in ICE measurements.

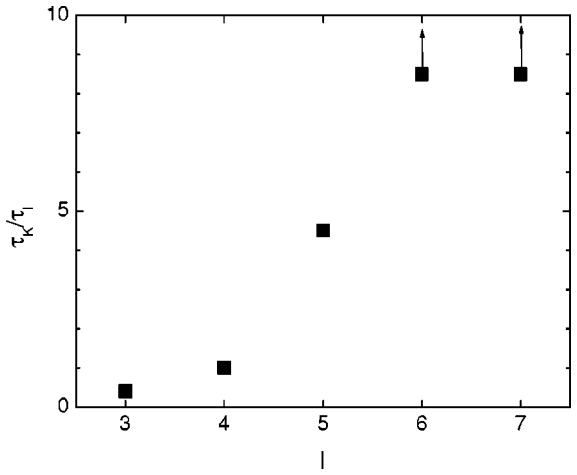

FIG. 8. Plots of the normalized autoionizing lifetime of the Sr $5p_{1/2}16l$ state by the $n=16$ Kepler period $\tau_K=0.623$ ps vs l.

IV. INTERPRETATION

The data of Fig. 7 show clearly that IEI becomes quite probable at $l=5$, for which the classical inner-turning point is $15a_0$, much smaller than the $55a_0$ inner-turning point of the states studied by Rosen *et al.* [5], but far larger than the $2.5a_0$ radius of the Sr^+5s core. Consequently, it is evident that the onset of IEI is not associated with penetration of the ionic core by the Rydberg electron.

We next consider the suggestion of Rosen *et al.* of the importance of electrostatic interactions. It is well known that electrostatic multipole interactions, primarily dipole and quadrupole, are responsible for autoionization of high-l states, and that autoionization rates fall rapidly with increasing l [10,15]. Stated another way, the lifetimes of autoionizing states increase rapidly with l. In Fig. 8 we plot the ratio of the lifetime τ_l of a Sr $5p_{1/2}16l$ state vs the $n=16$ Kepler period, $\tau_K=0.623$ ps. The lifetimes are obtained from the observed linewidths of the Sr $5s16l$-$5p_{1/2}16l$ transitions [10]. As shown, the ratio crosses 1 at $l=4$, which corresponds approximately to the onset of IEI shown in Fig. 7. Perhaps it is just a coincidence that the ratio of autoionization decay time relative to the Kepler time crosses 1 at the same l at which IEI becomes important, but it seems more likely that both autoionization and IEI are governed by long-range electrostatic interactions. In other words, the outer electron does not necessarily have to penetrate the core to inhibit IEI. The long-range interaction of the two electrons during the laser pulse can also lead to the ejection of the Rydberg electron.

V. SUMMARY

We have observed IEI vs l for Sr $5s16l$ atoms exposed to a 230-fs laser pulse, and we have observed that the probability of IEI is ~ 1 for $l>5$. Since this value of l is approximately the value for which the autoionization decay time matches the Kepler period, we infer that the long-range electrostatic interaction between the two-valence electrons governs whether or not IEI occurs.

ACKNOWLEDGMENTS

This work has been supported by the U.S. Department of Energy, Grant No. DEFG02-97ER14786. We are pleased to acknowledge valuable suggestions from R.R. Jones.

[1] H. Stapelfeldt, D.G. Papaioannou, L.D. Noordam, and T.F. Gallagher, Phys. Rev. Lett. **67**, 3223 (1991).
[2] R.R. Jones and P.H. Bucksbaum, Phys. Rev. Lett. **67**, 3215 (1991).
[3] H. Maeda, W. Li, and T.F. Gallagher, Phys. Rev. Lett. **85**, 5078 (2000).
[4] D.A. Tate and T.F. Gallagher, Phys. Rev. A **58**, 3058 (1998).
[5] C. Rosen, M. Dörr, U. Eichmann, and W. Sandner, Phys. Rev. Lett. **83**, 4514 (1999).
[6] T. F. Gallagher, *Rydberg Atoms* (Cambridge University Press, Cambridge, England, 1994).
[7] Richard R. Freeman and Daniel Kleppner, Phys. Rev. A **14**, 1614 (1976).
[8] C. E. Moore, *Atomic Energy Levels*, Natl. Bur. Stand. (U. S.) Circ. No. 467 (U. S. GPO, Washington, D. C., 1958), Vol. II, p. 189.
[9] P. Esherick, Phys. Rev. A **15**, 1920 (1977).
[10] W.E. Cooke, T.F. Gallagher, S.A. Edelstein, and R.M. Hill, Phys. Rev. Lett. **40**, 178 (1978).
[11] Michael G. Littman and Harold J. Metcalf, Appl. Opt. **17**, 2224 (1978).
[12] M.G. Littman, Opt. Lett. **3**, 128 (1978).
[13] L. Pruvost, P. Camus, J-M. Lecomte, C.R. Mahon, and P. Pillet, J. Phys. B **24**, 4723 (1991).
[14] T.F. Gallagher, R. Kachru, and N.H. Tran, Phys. Rev. A **26**, 2611 (1982).
[15] R.R. Jones and T.F. Gallagher, Phys. Rev. A **38**, 2846 (1988).